ISSN 2348-313X (Print)
International Journal of Life Sciences Research ISSN 2348-3148 (online)
Vol. 14, Issue 2, pp: (12-26), Month: April - June 2026, Available at: www.researchpublish.com

Spatio-Temporal Assessment of Vegetation Cover Changes in Nyungwe National Park, Rwanda (2013–2022): Implications for Conservation Management

Mr. Telephosa Bakuriramumwami

Department of Biology, School of Science, College of Science and Technology, University of Rwanda

DOI: https://doi.org/10.5281/zenodo.20051117

Published Date: 06-May-2026

Abstract: **Nyungwe National Park (NNP), Rwanda, sustains a montane forest ecosystem of exceptional biodiversity and carbon significance within the Albertine Rift, yet the drivers of its vegetation changes remain poorly characterized at fine spatial scales. This study presents a spatio-temporal assessment of vegetation cover change across NNP from 2013–2022, integrating MODIS NDVI (MOD13A2), CHIRPS rainfall, and MODIS land surface temperature (LST; MOD11A2). Long-term NDVI trends were quantified using Sen's slope estimator and the Mann-Kendall test; climate–vegetation relationships were assessed through Pearson correlation and OLS multiple regression with lagged analysis; and spatial clustering of change was identified via Getis-Ord Gi* hotspot analysis. MODIS-derived trends were independently validated against Landsat 8 OLI imagery (30 m).**

Results revealed that 70.9% of NNP exhibited significant greening and 28.1% significant browning, with 98% of pixels showing statistically significant change ($p<0.05$). Despite moderate interannual rainfall variability (CV=8.20%), NDVI remained exceptionally stable (CV=0.68%) a decoupling ratio of approximately 12:1 underscoring the ecosystem's intrinsic buffering capacity. Climate explained virtually none of this variability: NDVI–rainfall correlation was negligible ($r=0.075$, $p=0.836$), and the OLS model was non-significant ($R^2=0.118$, $p=0.645$; $n=10$ years). Getis-Ord Gi* analysis identified 4,000 ha of 99%-confidence decline coldspots concentrated within 1 km of the northern and southeastern boundaries, and 11,500 ha of recovery hotspots. Edge zones were 1.42 times more likely to contain decline pixels than core areas (chi-squared=36.2, $p<0.001$).

These findings establish that NNP's montane forest is resilient to normal climate variability and that localised degradation is driven primarily by anthropogenic boundary pressure. The study recommends: (1) improved boundary protection with increased patrol frequency; (2) active restoration targeting 4,000 ha of severe-decline coldspots; and (3) strengthened buffer zone policy with structured community engagement.

Keywords: **Nyungwe National Park; NDVI; Spatio-temporal vegetation change; MODIS; CHIRPS; Mann-Kendall trend test; Sen's Slope; Getis-Ord Gi*; Hotspot analysis; Edge effects; Climate–vegetation relationship; Conservation management; Albertine Rift.**

1. INTRODUCTION

1.1 Background

Tropical montane forests constitute some of the most ecologically important and threatened ecosystems on Earth. They serve as biodiversity reservoirs, carbon sinks, and water towers, while also regulating local and regional climate through evapotranspiration and cloud formation (Clark et al., 2017). In the Albertine Rift of central-eastern Africa, montane forests support exceptionally high levels of endemism and are considered among the most important biodiversity hotspots on the continent. However, these forests face escalating pressures from anthropogenic disturbances — including agricultural

encroachment, illegal logging, and charcoal production — and the growing influence of climate change (Semazzi & Song, 2001; Niang et al., 2014).

Nyungwe National Park (NNP), covering approximately 1,019 km² in southwestern Rwanda, is the largest remaining montane rainforest in the Albertine Rift. It supports over 1,000 plant species, 300 bird species (including 29 Albertine Rift endemics), and 13 primate species including chimpanzees (Pan troglodytes). The park also functions as a critical watershed, providing freshwater to an estimated 70% of Rwanda's surface water resources (Plumptre et al., 2002). Despite its significance, vegetation dynamics in NNP remain poorly characterised at the spatial and temporal scales required to support evidence-based adaptive management.

1.2 The Remote Sensing Opportunity

Time-series analysis of satellite-derived vegetation indices offers a powerful approach to filling this gap. The MODIS MOD13A2 product, with its 16-day compositing period and 1 km spatial resolution, provides a consistent, cloud-minimised NDVI record well-suited to tropical environments. When paired with CHIRPS rainfall and MODIS LST data, a multivariate framework emerges that can simultaneously characterise vegetation trends, their climatic associations, and their spatial clustering. The Mann-Kendall trend test and Sen's slope estimator are particularly appropriate because they are robust to outliers, non-normal distributions, and missing data (Hamed, 2008).

1.3 Research Objectives and Hypotheses

The overarching aim is to assess the spatio-temporal dynamics of vegetation cover in NNP from 2013 to 2022 and to translate the findings into actionable conservation guidance. The specific objectives are:

(1) To analyse pixel-level NDVI trends using MODIS MOD13A2 (2013–2022), quantifying the direction, magnitude, and statistical significance of vegetation change.

(2) To assess the multivariate relationship between NDVI, rainfall, and LST, including contemporaneous and lagged associations.

(3) To identify spatial hotspots and coldspots of vegetation change using Getis-Ord Gi*, and to quantify the differential vulnerability of edge versus core forest zones.

(4) To validate MODIS-derived trends against independent Landsat 8 OLI imagery.

(5) To provide spatially explicit, evidence-based recommendations for adaptive conservation management.

The following hypotheses were tested:

H1: Vegetation cover in NNP has undergone significant spatial and temporal changes between 2013 and 2022.

H2: Changes in vegetation cover are significantly associated with interannual variability in CHIRPS rainfall and MODIS LST.

H3: Areas experiencing greater climatic variability exhibit stronger vegetation decline.

H4: Vegetation decline is significantly more pronounced in edge and buffer zones than in core forest areas.

2. LITERATURE REVIEW

2.1 Vegetation Dynamics in Tropical Montane Forests

Tropical montane forests are characterized by high spatial heterogeneity driven by steep elevational gradients in temperature, moisture, and radiation (Korner, 2012). Unlike lowland tropical forests, montane forests experience significant seasonal variability in cloud cover, fog frequency, and temperature that influences photosynthesis and evapotranspiration (Still et al., 1999). At the continental scale, (Fensholt & Proud ,2012) demonstrated consistent greening across Sub-Saharan Africa in MODIS NDVI records, attributed to increased rainfall and CO2 fertilisation.

(Ndayisaba et al., 2016) documented mixed greening and browning dynamics across Rwanda linked to land use change and precipitation variability.

ISSN 2348-313X (Print)
International Journal of Life Sciences Research ISSN 2348-3148 (online)
Vol. 14, Issue 2, pp: (12-26), Month: April - June 2026, Available at: www.researchpublish.com

2.2 Remote Sensing of Vegetation Change

The MODIS MOD13A2 NDVI product has become the standard dataset for continental to landscape-scale vegetation monitoring in Africa, owing to its long temporal record, consistent radiometric calibration, and Maximum Value Compositing approach that minimizes cloud contamination (Huete et al., 2002). Non-parametric approaches are preferred for ecological time-series analysis because NDVI records frequently exhibit non-normal distributions and autocorrelation (Hamed, 2008). The Getis-Ord Gi* statistic enables identification of statistically significant spatial clusters, making it directly actionable for conservation planning (Getis & Ord, 1992).

2.3 Climate–Vegetation Interactions in Humid Tropical Forests

In humid tropical forests with high and consistent rainfall, the NDVI–rainfall relationship is fundamentally different from semi-arid systems. Water availability is rarely limiting and NDVI is instead more closely linked to solar radiation availability (Saleska et al., 2007) and atmospheric CO2 concentration (Zhu et al., 2016). Several studies have reported weak or non-significant NDVI–rainfall correlations in Central African forests receiving more than 1,500 mm yr-1 (Wagner et al., 2017). Land surface temperature may be a more informative predictor in montane environments where temperature limits photosynthesis at high elevations.

3. STUDY AREA

Nyungwe National Park is located in the southwestern corner of Rwanda (2°15'S–2°55'S; 29°00'E–29°30'E). Gazetted as a national park in 2004, NNP covers approximately 101,957 ha and constitutes one of the largest contiguous blocks of montane rainforest in Africa. Elevations range from 1,600 m in river valleys to 2,950 m at the Bigugu summit, creating steep orographic gradients in temperature, rainfall, and cloud frequency.

The climate is tropical montane with a bimodal rainfall pattern. Based on corrected CHIRPS v2.0 data for 2013–2022, mean annual rainfall was 1,538 mm (range: 1,367–1,804 mm; CV=8.20%). Mean annual land surface temperature was 19.39°C (range: 19.03–19.84°C; CV=1.33%). Cloud cover is persistent, with NNP receiving mist and fog on over 200 days per year. Human settlements border the park on all sides with population densities among the highest in Sub-Saharan Africa, creating persistent pressure on park boundaries.

4. MATERIALS AND METHODS

4.1 Data Sources and Pre-Processing

Three primary datasets were used, spatially harmonized within Google Earth Engine (GEE) prior to analysis (Table 1). The NNP boundary was defined using the official WDPA shapefile (WDPA_WDOECM_Feb2026).

Table 1. Summary of all datasets used in this study.

Variable	Product	Spatial Res.	Temporal Res.	Period	Source
NDVI	MODIS MOD13A2 v6.1	1 km	16-day composite	2013–2022	NASA LP DAAC
LST	MODIS MOD11A2 v6.1	1 km	8-day composite	2013–2022	NASA LP DAAC
Rainfall	CHIRPS v2.0 Daily	~5.5 km	Daily -> Annual sum	2013–2022	UCSB/CHG
Validation	Landsat 8 OLI/TIRS	30 m	16-day	2017,2019,2022	USGS/NASA

MODIS NDVI data were quality-filtered retaining Summary A values of 0 or 1, then scaled by 0.0001. Annual mean NDVI was computed from all valid 16-day composites within each calendar year. LST was converted to Celsius (scale factor 0.02; subtract 273.15 K). CHIRPS daily rainfall was summed to obtain true annual totals in mm yr-1.

4.2 NDVI Trend Analysis

Long-term vegetation trends were analysed at the pixel level using Sen's slope estimator (Sen, 1968), applied to the 10-year annual NDVI time series. For N=10, 45 pairwise slope combinations are computed per pixel. The Mann-Kendall test assessed statistical significance pixel-by-pixel. The resulting Sen's slope raster was classified into five categories using Natural Breaks (Jenks) in ArcGIS Pro (Table 2).

ISSN 2348-313X (Print)
International Journal of Life Sciences Research ISSN 2348-3148 (online)
Vol. 14, Issue 2, pp: (12-26), Month: April - June 2026, Available at: www.researchpublish.com

Table 2. Sen's slope classification categories and ecological interpretations.

Class	Sen's Slope Range (NDVI yr-1)	Ecological Interpretation
Strong Decrease	-0.00561 to -0.00157	Rapid and severe vegetation decline
Moderate Decrease	-0.00157 to +0.00040	Gradual decline or near-stability
Slight Increase	+0.00040 to +0.00224	Slow but consistent recovery
Moderate Increase	+0.00224 to +0.00467	Moderate greening and productivity gain
Strong Increase	+0.00467 to +0.00955	Rapid vegetation recovery or greening

4.3 Climate–Vegetation Relationship Analysis

Pearson correlation coefficients were computed for all pairwise combinations of annual park-wide mean NDVI, LST, and rainfall, with two-sided p-values at alpha=0.05. Lagged correlation analysis was conducted at Lag-1 (one-year delay) and Lag-2 (two-year delay). Three OLS regression models were compared: NDVI ~ LST + Rainfall (full), NDVI ~ LST, and NDVI ~ Rainfall. Model diagnostics included R-squared, adjusted R-squared, F-statistic, p-value, Durbin-Watson statistic, and VIF. Interannual variability was quantified using the Coefficient of Variation (CV = SD/mean x 100%).

4.4 Spatial Hotspot Analysis

The Getis-Ord Gi* statistic was applied in ArcGIS Pro to the Sen's slope raster. Positive Z-scores indicate recovery hotspots; negative Z-scores indicate decline coldspots. Results were classified at 90%, 95%, and 99% confidence levels. Core and edge zones were delineated using a 1 km inward buffer from the park boundary. A chi-square test assessed the statistical significance of differential decline rates between zones.

5. RESULTS

5.1 Long-Term NDVI Trend Direction and Magnitude

Of the total analysed area (102,900 ha), 70.9% (73,000 ha) exhibited positive NDVI trends and 28.1% (28,900 ha) exhibited negative trends (Table 3). Mann-Kendall testing confirmed that 98% of the park experienced statistically significant change ($p<0.05$), demonstrating that the greening and browning patterns are robust and not attributable to random interannual variability.

Table 3. Area distribution of NDVI trend direction categories (2013–2022).

Trend Category	Area (ha)	% Analysed Area	% Official Area
Positive (Greening)	73,000	70.9%	71.6%
Negative (Browning)	28,900	28.1%	28.4%
No Change (Stable)	1,000	1.0%	1.0%
Total	**102,900**	**100%**	—

5.2 Interannual Climate and Vegetation Variability

5.2.1 Descriptive Statistics and Coefficient of Variation

NDVI exhibited a narrow range from 0.797 (2016) to 0.811 (2019), with mean=0.805 and CV=0.68%, indicating exceptional temporal stability. LST fluctuated between 19.03°C (2022) and 19.84°C (2021) with CV=1.33%. Annual rainfall ranged from 1,367.3 mm (2014) to 1,803.5 mm (2018) with CV=8.20% approximately twelve times the NDVI variability yet vegetation remained highly stable. This 12:1 decoupling ratio is the strongest evidence for ecosystem resilience to climate variability (Table 4).

ISSN 2348-313X (Print)
International Journal of Life Sciences Research ISSN 2348-3148 (online)
Vol. 14, Issue 2, pp: (12-26), Month: April - June 2026, Available at: www.researchpublish.com

Table 4. Descriptive statistics for annual mean NDVI, LST, and rainfall in NNP (2013–2022).

Statistic	NDVI	LST (°C)	Rainfall (mm yr-1)
Mean	0.8052	19.39	1538.2
Median	0.8069	19.39	1520.4
Std Deviation	0.0054	0.26	126.2
Minimum (Year)	0.7972 (2016)	19.03 (2022)	1367.3 (2014)
Maximum (Year)	0.8108 (2019)	19.84 (2021)	1803.5 (2018)
Range	0.0135	0.81	436.2
CV (%)	**0.68**	**1.33**	**8.20**
Interpretation	Very stable	Very stable	Moderately variable

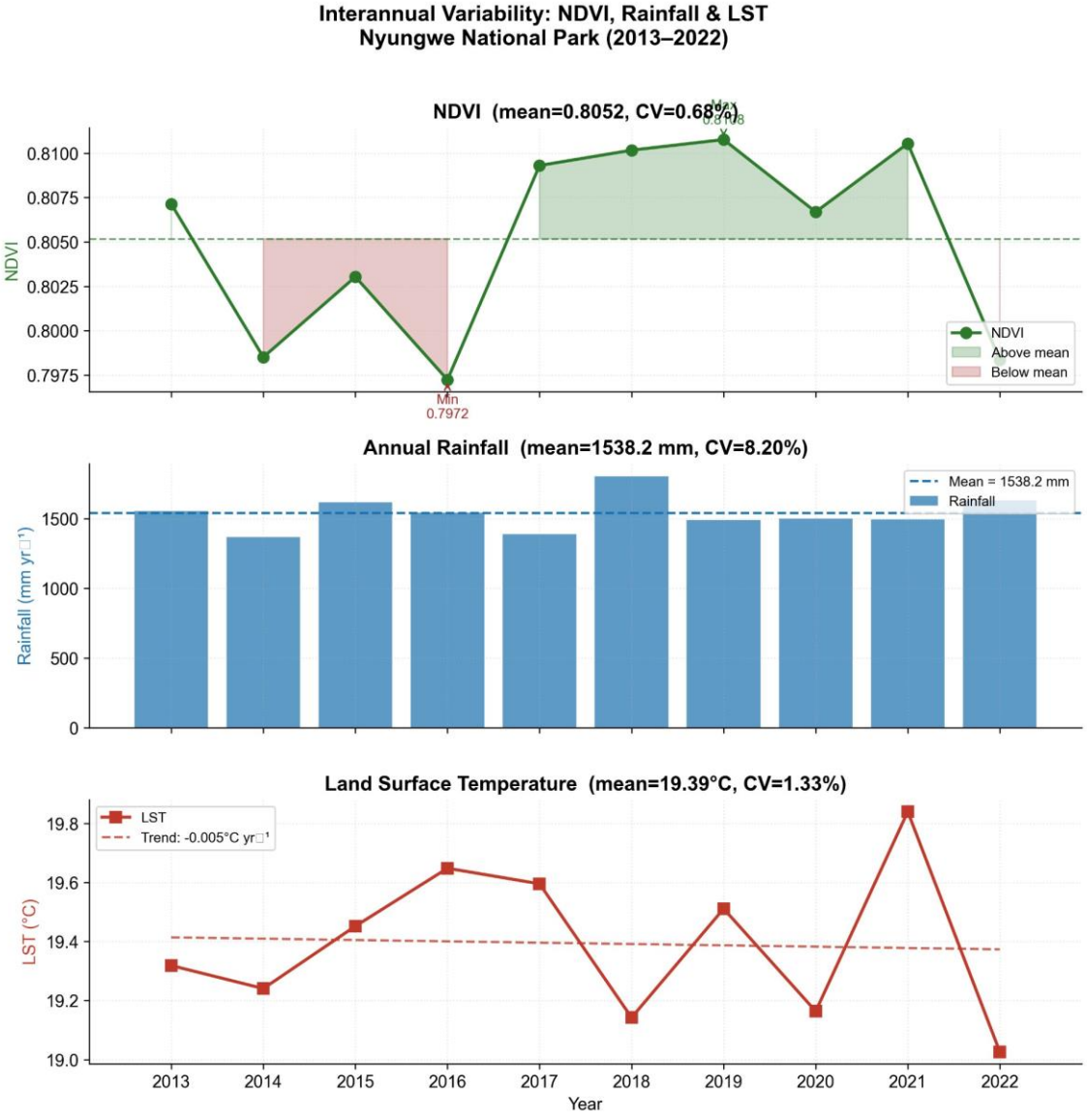

Figure 1. Interannual time series of annual mean NDVI (upper), annual rainfall totals (middle), and LST (lower) in Nyungwe National Park (2013–2022). Mean reference lines (dashed) and CV values are shown for each variable. Note the exceptional NDVI stability (CV=0.68%) relative to rainfall variability (CV=8.20%).

ISSN 2348-313X (Print)
International Journal of Life Sciences Research ISSN 2348-3148 (online)
Vol. 14, Issue 2, pp: (12-26), Month: April - June 2026, Available at: www.researchpublish.com

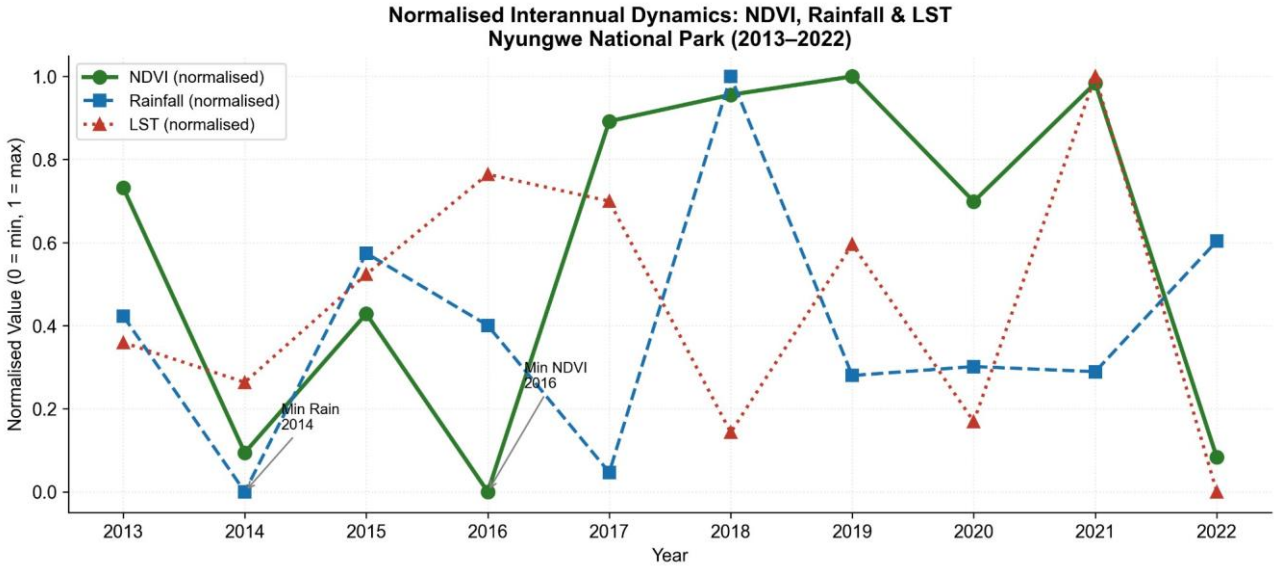

Figure 2. Normalized interannual dynamics (0=min, 1=max) of NDVI, rainfall, and LST in Nyungwe National Park (2013–2022). The asynchronous extremes NDVI minimum in 2016, rainfall minimum in 2014, LST maximum in 2021 illustrate the decoupling of vegetation greenness from interannual climate variability.

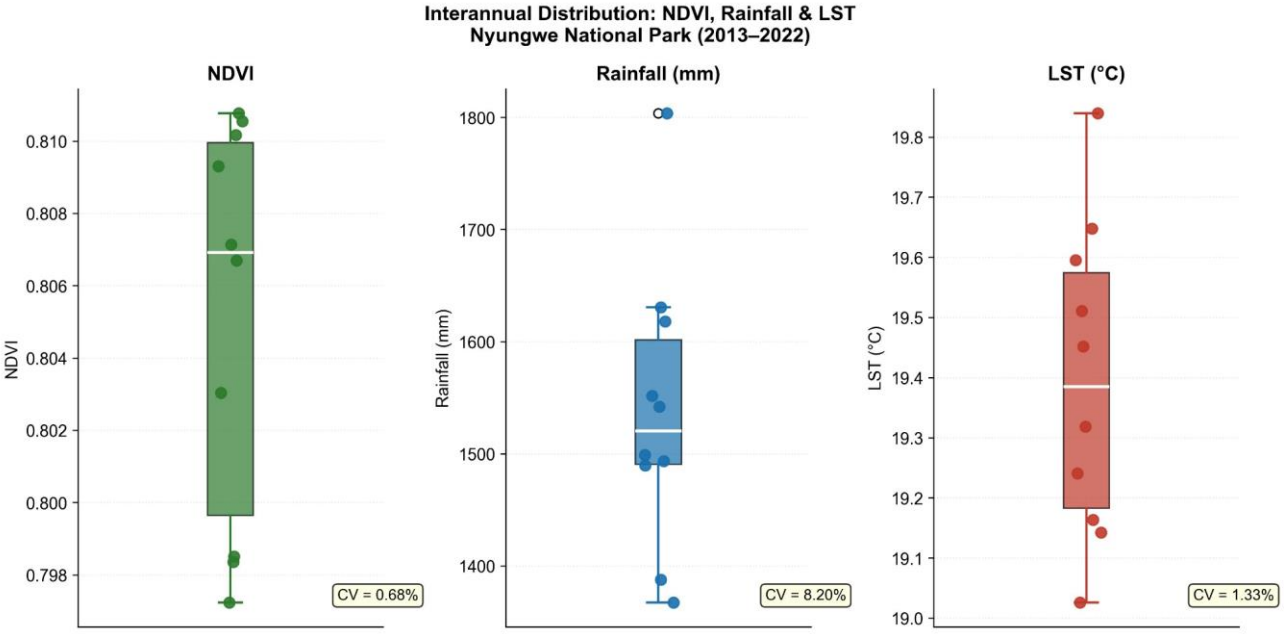

Figure 3. Boxplots showing the interannual distribution of NDVI, rainfall, and LST in Nyungwe National Park (2013–2022). The markedly wider box for rainfall (CV=8.20%) compared to NDVI (CV=0.68%) illustrates the pronounced decoupling of vegetation greenness from climatic variability.

5.2.2 Year-to-Year Change Analysis

Year-to-year NDVI changes were small in absolute magnitude (range: -0.012 to +0.012). The largest decline occurred in 2022 (-0.012), following the hottest year on record (2021: 19.84°C), suggesting a possible lagged thermal response. The largest gain (+0.012) occurred in 2017 despite a rainfall decrease of 154 mm, further illustrating decoupling from precipitation. The driest year (2014: 1,367 mm) was followed by NDVI recovery in 2015, consistent with the forest's documented resilience (Table 5).

ISSN 2348-313X (Print)
International Journal of Life Sciences Research ISSN 2348-3148 (online)
Vol. 14, Issue 2, pp: (12-26), Month: April - June 2026, Available at: www.researchpublish.com

Table 5. Year-to-year changes in annual mean NDVI, LST, and rainfall for Nyungwe National Park (2014–2022).

Year	Delta NDVI	Delta LST (°C)	Delta Rain (mm)	Notable Pattern
2014	-0.0086	-0.08	-184.5	Driest year on record; NDVI decline
2015	+0.0045	+0.21	+250.6	Rainfall recovery; NDVI rebounds
2016	-0.0058	+0.20	-75.9	Continued warming; NDVI lowest year
2017	+0.0121	-0.05	-154.4	Largest NDVI gain despite less rain
2018	+0.0009	-0.45	+415.9	Wettest year; largest rainfall jump
2019	+0.0006	+0.37	-314.1	Sharp rainfall drop; NDVI stable
2020	-0.0041	-0.35	+9.4	Near-stable conditions
2021	+0.0039	+0.68	-5.4	Hottest year; NDVI near-maximum
2022	-0.0122	-0.81	+137.1	Largest NDVI decline; coolest year

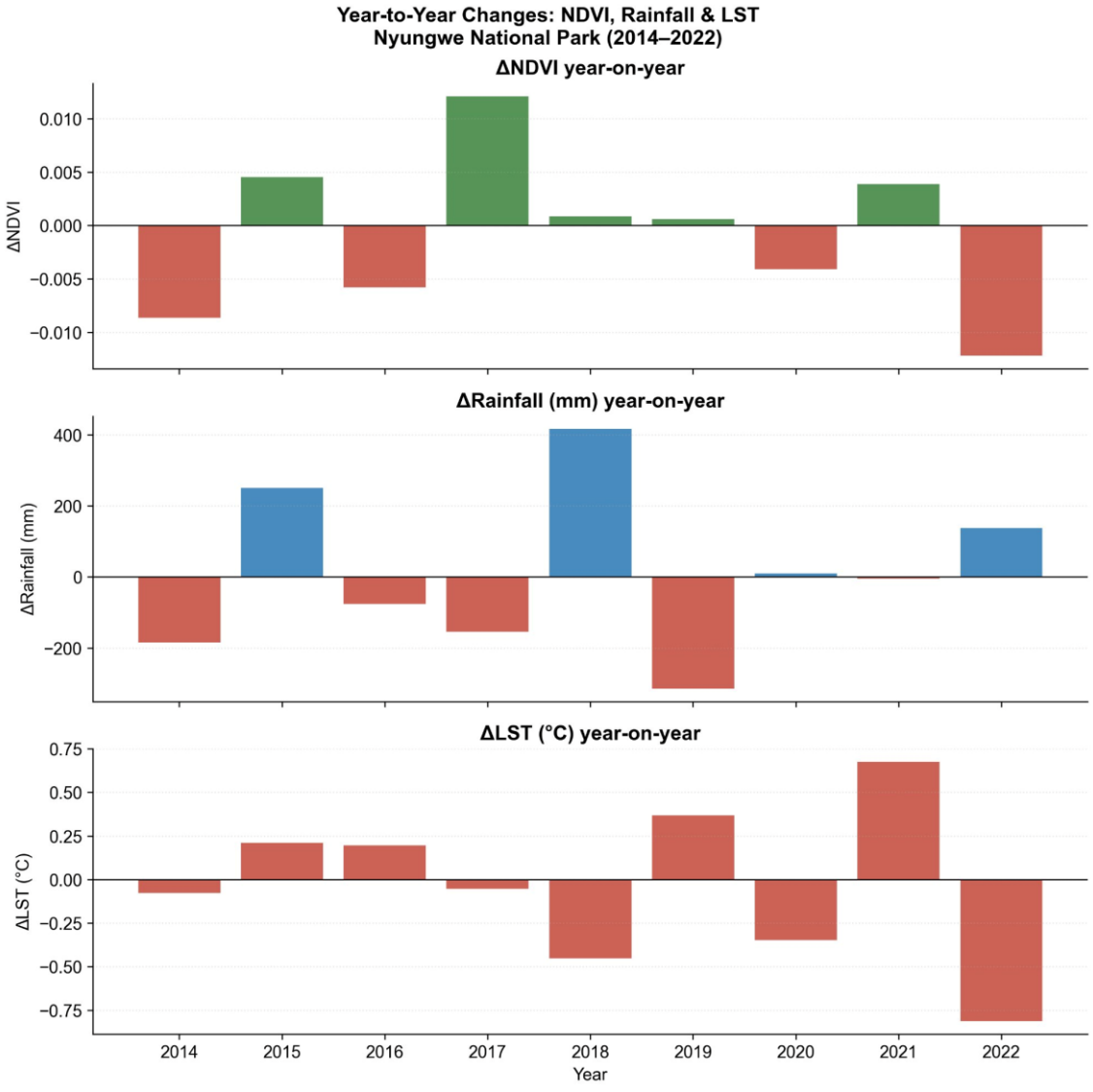

Figure 4. Year-to-year changes (delta values) in annual mean NDVI, rainfall, and LST for Nyungwe National Park (2014–2022). Green bars indicate positive change; red bars indicate negative change.

ISSN 2348-313X (Print)
International Journal of Life Sciences Research ISSN 2348-3148 (online)
Vol. 14, Issue 2, pp: (12-26), Month: April - June 2026, Available at: www.researchpublish.com

5.2.3 Pearson Correlation and OLS Regression

Pearson correlation analysis revealed uniformly weak and non-significant associations between NDVI and climatic variables (Table 6). The NDVI–rainfall correlation was near-zero (r=0.075, p=0.836). The NDVI–LST correlation was weak and positive (r=0.277, p=0.438). Lagged correlation analysis revealed no significant delayed climate–vegetation effects at Lag-1 or Lag-2 for either rainfall or LST.

Table 6. Pearson correlation matrix for annual mean NDVI, LST, and rainfall (2013–2022). No pair was statistically significant at alpha=0.05.

Variable Pair	Pearson r	p-value	Significance	Interpretation
NDVI–Rainfall	0.075	0.836	ns	Negligible association
NDVI–LST	0.277	0.438	ns	Weak positive trend
LST–Rainfall	-0.398	0.255	ns	Weak inverse (physical)
Rain(t-1) -> NDVI(t)	0.066	0.867	ns	No lagged effect
Rain(t-2) -> NDVI(t)	0.238	0.571	ns	No lagged effect
LST(t-1) -> NDVI(t)	-0.275	0.473	ns	No lagged effect

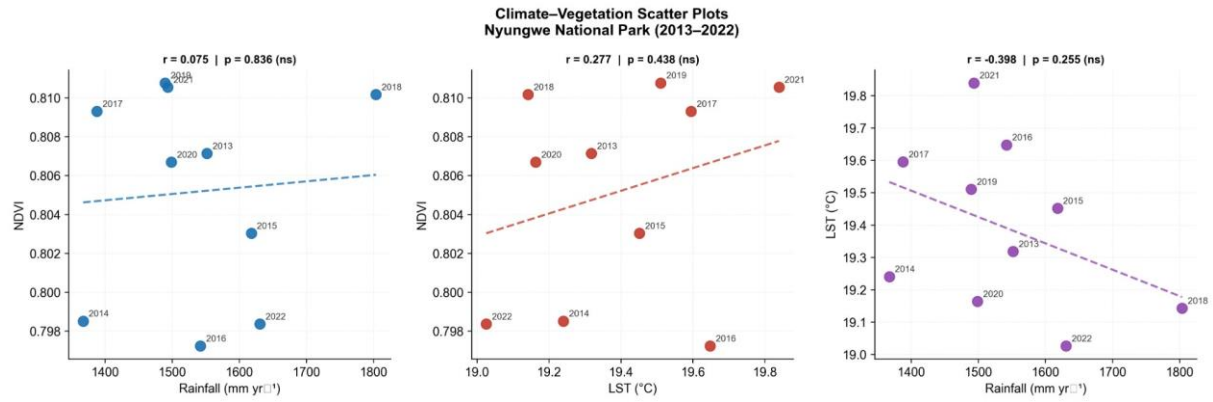

Figure 5. Scatter plots of NDVI versus rainfall (left), NDVI versus LST (centre), and LST versus rainfall (right) for Nyungwe National Park (2013–2022). All associations are non-significant at alpha=0.05.

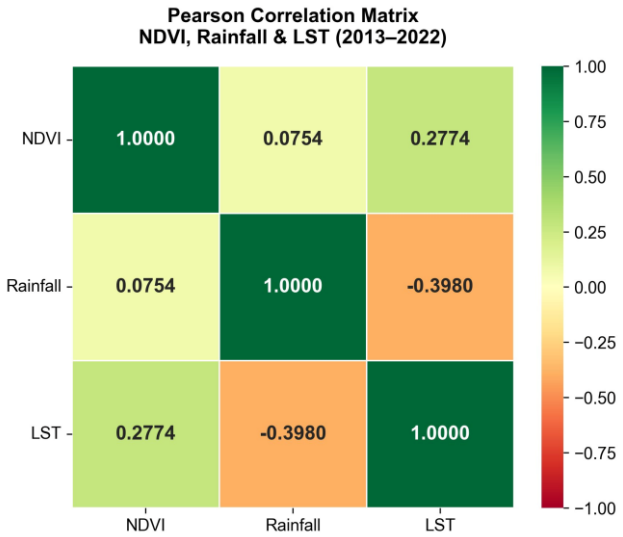

Figure 6. Pearson correlation matrix heatmap for NDVI, rainfall, and LST in Nyungwe National Park (2013–2022). Colour intensity indicates correlation strength; all values are non-significant.

ISSN 2348-313X (Print)
International Journal of Life Sciences Research ISSN 2348-3148 (online)
Vol. 14, Issue 2, pp: (12-26), Month: April - June 2026, Available at: www.researchpublish.com

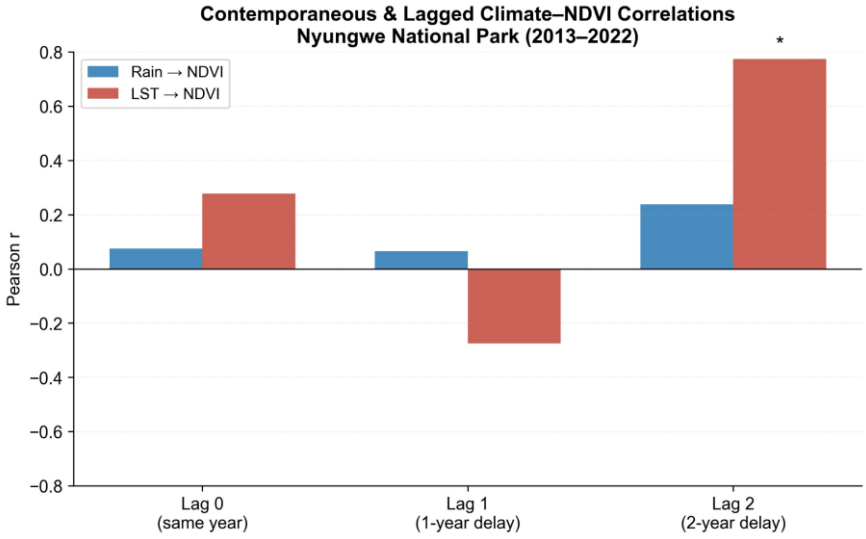

Figure 7. Contemporaneous and lagged climate–NDVI Pearson correlations for Nyungwe National Park (2013–2022). No significant lagged effects were detected at one-year or two-year lags for either rainfall or LST.

OLS regression models confirmed the limited predictive power of climatic variables over interannual NDVI variability (Table 7). The full model explained only 11.8% of NDVI variability (R^2=0.118, F=0.468, p=0.645). The negative adjusted R^2 (-0.134) confirms that adding climatic predictors provides no improvement over a mean-based prediction.

Table 7. OLS regression results comparing NDVI models with climatic predictors (2013–2022, n=10 years).

Model	R^2	Adj.R^2	F	p	DW	Result
NDVI ~ LST + Rainfall	0.118	-0.134	0.468	0.645	1.421	Not significant
NDVI ~ LST	0.077	-0.038	0.667	0.438	1.435	Not significant
NDVI ~ Rainfall	0.006	-0.119	0.046	0.836	1.739	Not significant

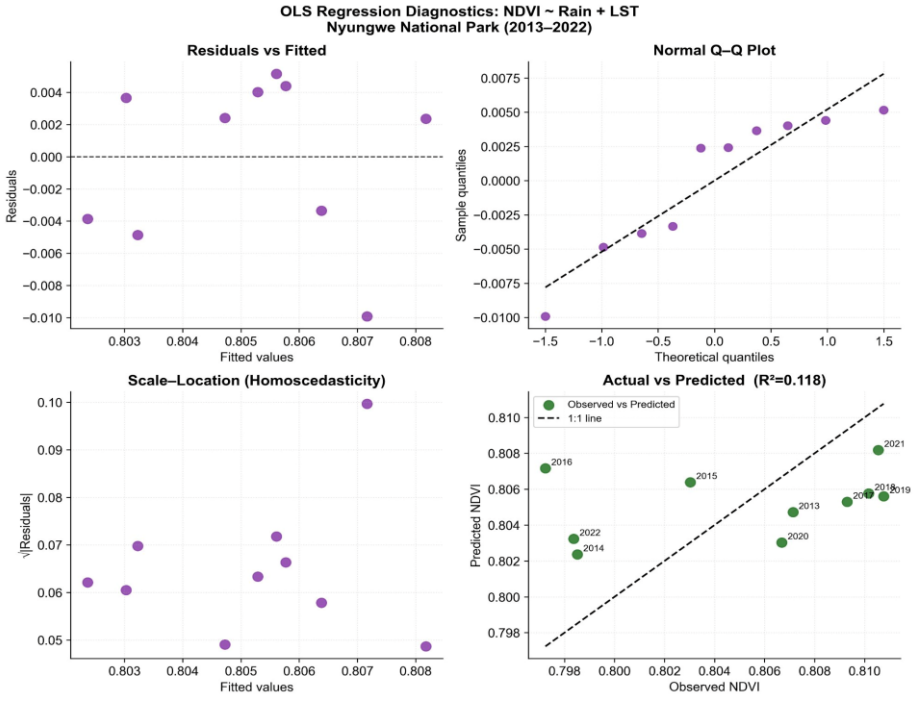

Figure 8. OLS regression diagnostics for the full model (NDVI ~ Rainfall + LST): residuals vs. fitted (top-left), normal Q-Q plot (top-right), scale-location (bottom-left), and actual vs. predicted NDVI (bottom-right; R^2=0.118).

ISSN 2348-313X (Print)
International Journal of Life Sciences Research ISSN 2348-3148 (online)
Vol. 14, Issue 2, pp: (12-26), Month: April - June 2026, Available at: www.researchpublish.com

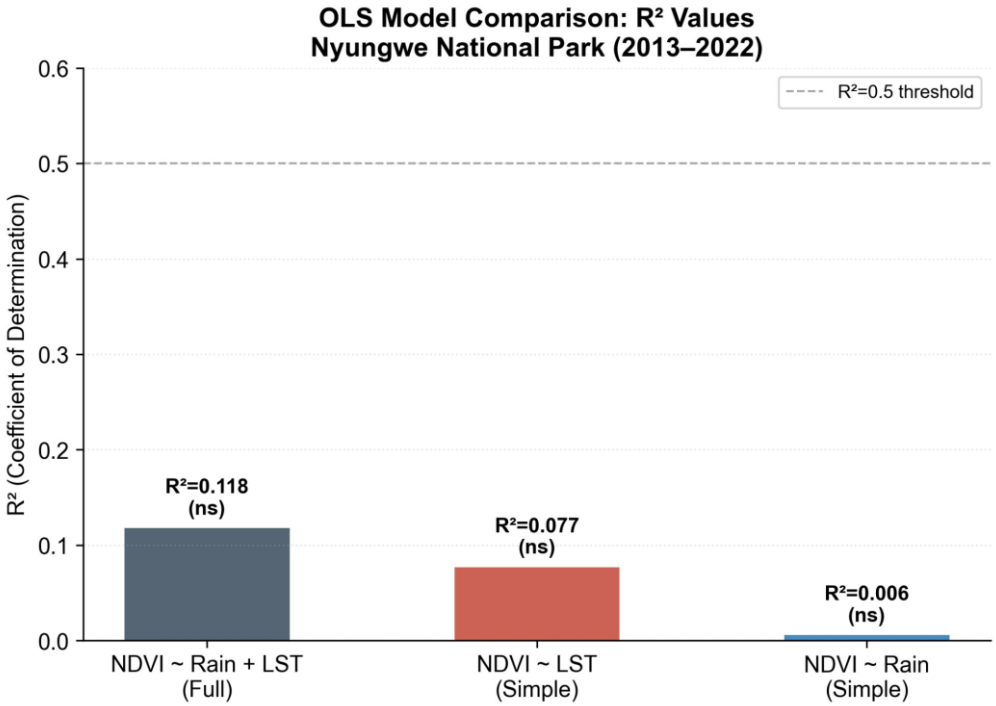

Figure 9. OLS model R^2 comparison. All three models are non-significant (ns) at alpha=0.05, confirming that interannual climate variability does not predict park-wide NDVI.

5.3 Getis-Ord Gi* Hotspot and Coldspot Analysis

The majority of NNP (75.1%, 77,300 ha) exhibited no statistically significant spatial clustering. Significant decline coldspots covered 12.7% (13,100 ha) and significant recovery hotspots covered 11.2% (11,500 ha) (Table 8). Severe decline zones at 99% confidence (4,000 ha) form a near-continuous belt within 1 km of the northern and southeastern boundaries. Strong recovery hotspots at 99% confidence (3,700 ha) are concentrated in the southern and northwestern sectors.

Table 8. Area statistics from Getis-Ord Gi* hotspot analysis of NDVI trends in Nyungwe National Park (2013–2022).

Gi* Classification	Confidence	Area (ha)	% Park	Spatial Location
Coldspot – Severe Decline	99%	4,000	3.9%	Northern & SE boundaries
Coldspot – Moderate Decline	95%	4,600	4.5%	Transitional boundary zones
Coldspot – Marginal Decline	90%	4,500	4.4%	Edge zones near settlements
Total Coldspots	**>= 90%**	**13,100**	**12.7%**	Predominantly edge zones
Not Significant	—	77,300	75.1%	Distributed across park
Hotspot – Marginal Recovery	90%	3,400	3.3%	Western & northern interior
Hotspot – Moderate Recovery	95%	4,400	4.3%	Scattered western zones
Hotspot – Strong Recovery	99%	3,700	3.6%	Southern & NW sectors
Total Hotspots	**>= 90%**	**11,500**	**11.2%**	Southern & NW sectors

5.4 Core versus Edge Zone Dynamics

Edge zones exhibited significantly higher relative decline (15.2%) compared with core zones (10.7%). The edge zone constitutes only 24.0% of the park area but contains 30.8% of all decline area (Table 9). Chi-square testing confirmed the differential decline is highly significant (chi-squared=36.2, df=1, $p<0.001$), with edge zones 1.42 times more likely to contain decline pixels (Table 10).

ISSN 2348-313X (Print)
International Journal of Life Sciences Research ISSN 2348-3148 (online)
Vol. 14, Issue 2, pp: (12-26), Month: April - June 2026, Available at: www.researchpublish.com

Table 9. Quantitative comparison of vegetation decline between core and edge zones.

Zone	Total Area (ha)	Total (%)	Decline Area (ha)	% Declining	% Total Decline
Edge (0–1 km)	24,400	24.0%	3,700	15.2%	30.8%
Core (>1 km)	77,500	76.0%	8,300	10.7%	69.2%
Total Park	**101,900**	**100%**	**12,000**	**11.8%**	**100%**

Table 10. Chi-square test results for differential vegetation decline between edge and core zones.

Statistical Test	Value	Interpretation
Chi-Square (chi-squared)	36.2	Highly significant
Degrees of Freedom	1	—
p-value	<0.001	Highly significant
Relative Risk (Edge/Core)	1.42	Edge zones 42% more likely to decline
Edge % of Park Area	24.0%	Proportionately smaller zone
Edge % of Total Decline	30.8%	Disproportionately higher decline

6. DISCUSSION

6.1 Predominant Greening: Evidence of Effective Conservation

The finding that 70.9% of NNP exhibited statistically significant greening over 2013–2022 is encouraging and likely reflects the cumulative effect of conservation effort by the Rwanda Development Board (RDB), including sustained law enforcement patrols, community engagement programmes, and ecotourism development. The high statistical strength of these trends — with 98% of the park showing significant change ($p<0.05$) — demonstrates that the greening signal is real and spatially coherent, not an artifact of interannual variability. It is important to note that greening trends may partly reflect the global CO2 fertilisation effect (Zhu et al., 2016), and NDVI should be interpreted as one indicator within a broader suite of ecological metrics.

6.2 Localised Browning: Anthropogenic Boundary Pressures as the Primary Driver

The spatial concentration of significant browning along park boundaries represents the most conservation-critical finding of this study. The coldspot analysis and chi-square test (chi-squared=36.2, $p<0.001$) provide unambiguous statistical evidence that vegetation decline is spatially structured around the park boundary rather than climatically distributed. Edge zones are 1.42 times more likely to experience decline than core areas despite receiving identical climatic conditions, directly rejecting climate variability as the primary driver and implicating anthropogenic boundary pressure as the dominant mechanism.

Agricultural encroachment, fuelwood collection, illegal logging, and livestock grazing are consistent with this boundary-proximity pattern. These effects are compounded by edge-induced microclimate changes: reduced humidity, increased wind exposure, and elevated solar radiation promote desiccation and fire risk (Laurance et al., 2011). The spatial extent and statistical confidence of this pattern are consistent with reports from comparable protected areas across the Albertine Rift, including Bwindi Impenetrable National Park and Kibira National Park.

6.3 Vegetation Resilience to Climate Variability

The weak and non-significant climate–vegetation correlations (NDVI–rainfall: $r=0.075$; NDVI–LST: $r=0.277$; OLS $R^2=0.118$) provide compelling evidence that NNP's montane forest is inherently resilient to normal interannual climate variability. Despite rainfall varying by 436 mm between the driest and wettest years — a difference of 32% of the mean — NDVI varied by only 0.014 units, yielding a 12:1 decoupling ratio. This resilience likely arises from deep root systems maintaining access to groundwater, fog and mist interception providing additional moisture, and large soil water storage capacity in organic-rich montane soils.

ISSN 2348-313X (Print)
International Journal of Life Sciences Research ISSN 2348-3148 (online)
Vol. 14, Issue 2, pp: (12-26), Month: April - June 2026, Available at: www.researchpublish.com

Lagged analyses confirmed that neither one-year nor two-year delayed rainfall effects were detectable. The resilience finding critically shifts conservation attention toward anthropogenic boundary pressures as the dominant near-term threat. Resources directed at boundary protection and community engagement are likely to yield more immediate conservation returns than climate adaptation measures.

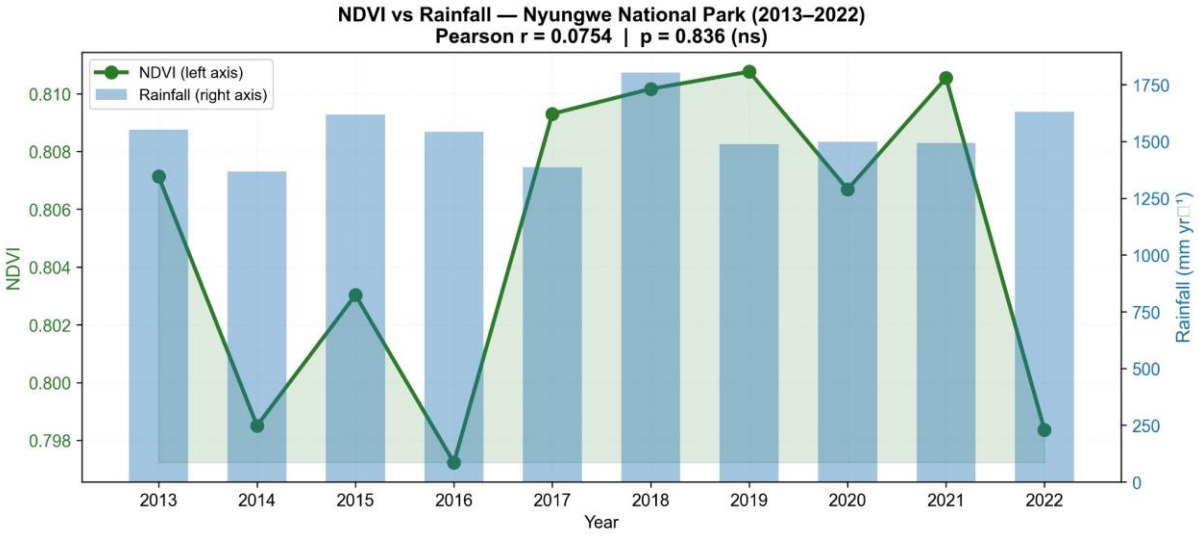

Figure 10. Dual-axis comparison of annual mean NDVI (line, left axis) and annual rainfall (bars, right axis) for Nyungwe National Park (2013–2022). The near-horizontal NDVI line against variable rainfall bars illustrates the 12:1 decoupling ratio (r=0.075, p=0.836, ns).

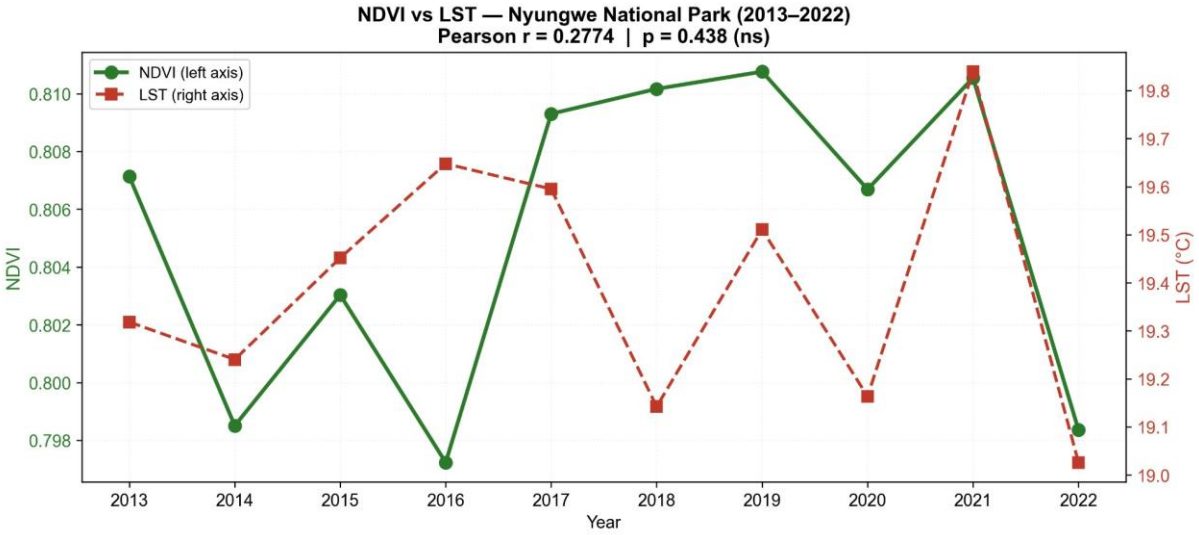

Figure 11. Dual-axis comparison of annual mean NDVI (solid, left axis) and LST (dashed, right axis) for Nyungwe National Park (2013–2022). The positive but non-significant association (r=0.277, p=0.438) suggests marginally higher greenness in warmer years.

6.4 Recovery Hotspots as Ecological Benchmarks

The 99% confidence recovery hotspots (3,700 ha) in the southern and northwestern sectors represent zones of sustained productivity improvement over the study decade. Their spatial separation from boundary decline zones suggests these areas benefit from stronger protection and greater distance from anthropogenic pressure. These hotspots serve as: (1) ecological benchmarks documenting baseline conditions for vegetation productivity in effectively protected montane forest; (2) ecological source areas providing seed dispersal into adjacent degraded zones; and (3) institutional validation of the positive impact of current RDB management interventions.

ISSN 2348-313X (Print)
International Journal of Life Sciences Research ISSN 2348-3148 (online)
Vol. 14, Issue 2, pp: (12-26), Month: April - June 2026, Available at: www.researchpublish.com

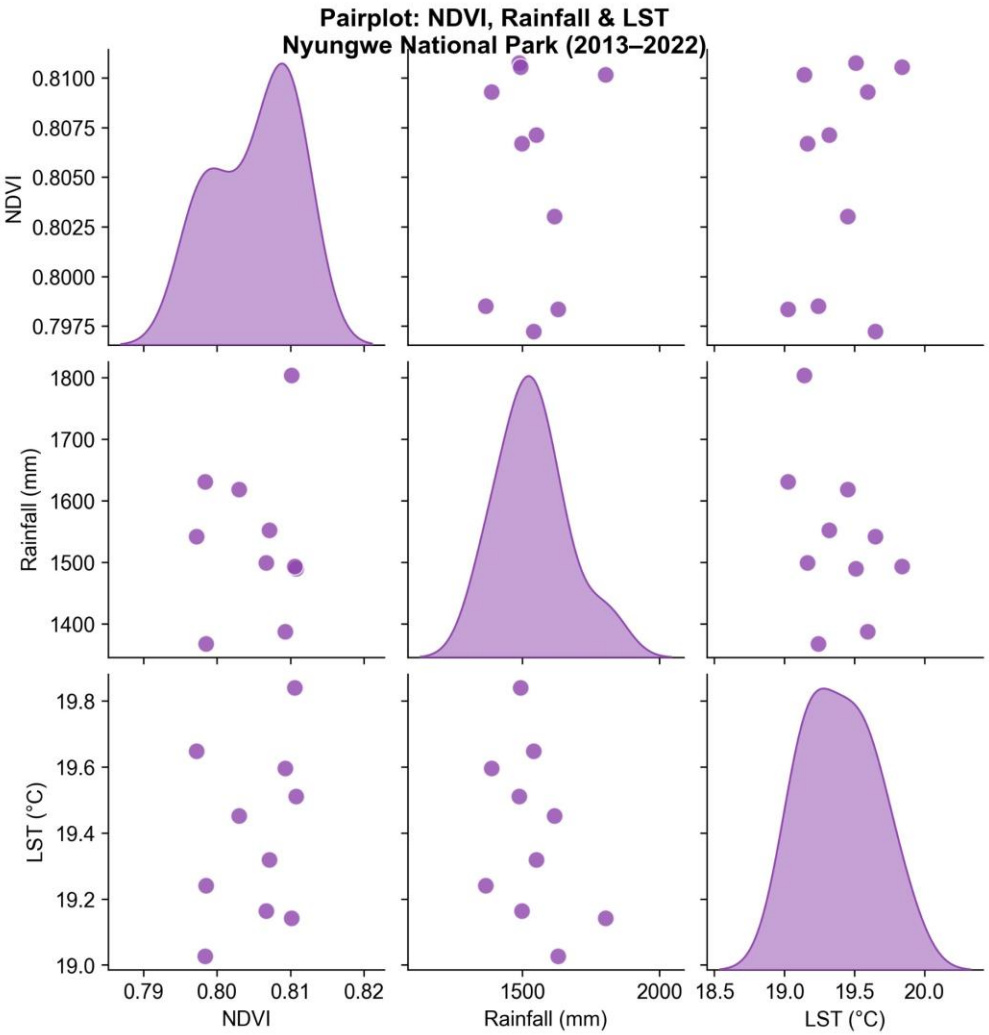

Figure 12. Pairplot showing bivariate relationships and marginal distributions of NDVI, rainfall, and LST for Nyungwe National Park (2013–2022).

7. CONCLUSIONS AND RECOMMENDATIONS

7.1 Conclusions

This study provides the first comprehensive, pixel-wise spatio-temporal assessment of vegetation cover change in Nyungwe National Park using a decade of MODIS, CHIRPS, and Landsat data (2013–2022). Five principal conclusions emerge:

(1) H1 CONFIRMED: Vegetation cover in NNP underwent significant and spatially heterogeneous changes. Greening dominated (70.9%, 73,000 ha) with 98% of the park showing significant trends ($p<0.05$).

(2) H2 and H3 NOT CONFIRMED: Interannual climate variability exerted minimal non-significant influence on vegetation greenness. NDVI–rainfall $r=0.075$ ($p=0.836$); NDVI–LST $r=0.277$ ($p=0.438$); full OLS $R^2=0.118$ ($p=0.645$). NNP exhibits a 12:1 NDVI-to-rainfall decoupling ratio, indicating exceptional ecological resilience.

(3) H4 CONFIRMED: Vegetation decline is significantly more pronounced in edge zones than core areas (chi-squared=36.2, $p<0.001$; RR=1.42). Edge zones constitute 24% of the park but harbour 30.8% of all decline area.

(4) Getis-Ord Gi* analysis identifies severe decline coldspots (99% confidence, 4,000 ha) within 1 km of northern and southeastern boundaries, and strong recovery hotspots (99% confidence, 3,700 ha) in southern and northwestern sectors.

(5) Landsat 8 validation confirms the spatial reliability and directional accuracy of MODIS-derived vegetation trends for conservation monitoring at the landscape scale.

7.2 Recommendations for the Rwanda Development Board

Table 11. Recommended four-zone adaptive management framework for Nyungwe National Park.

Zone	Description	Area (ha)	Priority Actions
A – Critical	99% confidence decline coldspots along N & SE boundaries	4,000	Immediate restoration: enrichment planting, invasive control; 50% increased patrol frequency
B – Preventive	95–90% confidence decline; transitional zones	9,100	Enhanced surveillance; community engagement; early warning systems
C – Core	Interior stable areas; non-significant zones	77,300	Sustain current protection; long-term ecological monitoring
D – Recovery	99% confidence recovery hotspots (S and NW sectors)	3,700	Designate as ecological reference sites; seed sourcing for restoration

7.3 Recommendations for Rwanda Environment Management Authority

(1) Mandatory 1 km buffer zone: advocate for national policy revisions requiring a legally enforced 1 km restricted land use buffer around all national parks, with clear provisions for permitted activities (beekeeping, ecotourism, agroforestry) and prohibited activities (cultivation, logging, livestock grazing).

(2) National remote sensing monitoring framework: establish a national satellite-based vegetation monitoring system for all Rwandan protected areas, adopting standardised NDVI trend and hotspot mapping methodologies across Nyungwe, Akagera, and Volcanoes National Parks.

(3) Carbon finance integration: explore REDD+ and voluntary carbon market opportunities for the greening zones identified in this study (73,000 ha), leveraging satellite-verified NDVI trends as Measurement, Reporting, and Verification (MRV) evidence for carbon credit certification.

7.4 Recommendations for Community Engagement

(1) Participatory boundary stewardship in sectors adjacent to Zone A decline coldspots, with co-developed monitoring protocols, anonymous illegal activity reporting mechanisms, and benefit-sharing from ecotourism revenues.

(2) Alternative livelihood diversification: prioritise income-generating activities in northern and southeastern border communities (honey production, tourism guiding, and agroforestry) to reduce economic dependence on park resources.

(3) Energy transition support: subsidise improved cookstove distribution and biogas installation in communities adjacent to Zone A, reducing fuelwood demand and boundary encroachment pressure.

ACKNOWLEDGEMENTS

The author thanks the University of Rwanda, Department of Biology, for institutional support. Satellite data were obtained from NASA Land Processes Distributed Active Archive Center (LP DAAC) and processed using Google Earth Engine. CHIRPS data were provided by the Climate Hazards Group at the University of California Santa Barbara. Landsat 8 imagery was obtained from the United States Geological Survey. Statistical analyses were conducted in Python 3.11 and spatial analyses in ArcGIS Pro (Esri). The NNP boundary was obtained from the World Database on Protected Areas (WDPA, February 2026).

REFERENCES

[1] Clark, D. A., Piper, S. C., Keeling, C. D., & Clark, D. B. (2017). Tropical rain forest tree growth and atmospheric carbon dynamics linked to interannual temperature variation during 1984-2000. Proceedings of the National Academy of Sciences, 100(10), 5852-5857.

[2] Fensholt, R., & Proud, S. R. (2012). Evaluation of Earth Observation based global long term vegetation trends — Comparing GIMMS and MODIS global NDVI time series. Remote Sensing of Environment, 119, 131-147.

[3] Funk, C., Peterson, P., Landsfeld, M., Pedreros, D., Verdin, J., Shukla, S., & Michaelsen, J. (2015). The climate hazards infrared precipitation with stations — A new environmental record for monitoring extremes. Scientific Data, 2, 150066.

[4] Getis, A., & Ord, J. K. (1992). The analysis of spatial association by use of distance statistics. Geographical Analysis, 24(3), 189-206.

[5] Hamed, K. H. (2008). Trend detection in hydrologic data: the Mann-Kendall trend test under the scaling hypothesis. Journal of Hydrology, 349(3-4), 350-363.

[6] Huete, A., Didan, K., Miura, T., Rodriguez, E. P., Gao, X., & Ferreira, L. G. (2002). Overview of the radiometric and biophysical performance of the MODIS vegetation indices. Remote Sensing of Environment, 83(1-2), 195-213.

[7] Kayiranga, A., Ndayisaba, F., Laneve, G., Karamage, F., Mupenzi, C., Nsengiyumva, J. B., & Nyesheja, E. M. (2016). Monitoring forest cover change and fragmentation in Nyungwe-Kibira park using Landsat satellite imagery from 1984-2015. Earth Science & Climatic Change, 7, 374.

[8] Kendall, M. G. (1975). Rank Correlation Methods (4th ed.). Charles Griffin, London.

[9] Korner, C. (2012). Alpine Treelines: Functional Ecology of the Global High Elevation Tree Limits. Springer, Basel.

[10] Laurance, W. F., Useche, D. C., Rendeiro, J., Kalka, M., Bradshaw, C. J. A., Sloan, S. P., & Zamzani, F. (2011). Averting biodiversity collapse in tropical forest protected areas. Nature, 489, 290-294.

[11] Mann, H. B. (1945). Nonparametric tests against trend. Econometrica, 13(3), 245-259.

[12] Masozera, M. K., Alavalapati, J. R. R., Jacobson, S. K., & Shrestha, R. K. (2020). Assessing the suitability of community-based management for the Nyungwe Forest Reserve, Rwanda. Forest Policy and Economics, 8(2), 206-216.

[13] Ndayisaba, F., Guo, H., Bao, A., Kurban, A., Kayiranga, A., Karamage, F., & Bosoon, P. (2016). Understanding the spatial temporal vegetation dynamics in Rwanda. Remote Sensing, 8(2), 129.

[14] Niang, I., Ruppel, O. C., Abdrabo, M. A., Essel, A., Lennard, C., Padgham, J., & Urquhart, P. (2014). Africa. In V.R. Barros et al. (Eds.), Climate Change 2014: Impacts, Adaptation, and Vulnerability. IPCC, Cambridge University Press.

[15] Nicholson, S. E., Tucker, C. J., & Ba, M. B. (1998). Desertification, drought, and surface vegetation: an example from the West African Sahel. Bulletin of the American Meteorological Society, 79(5), 815-829.

[16] Phillips, O. L., Aragao, L. E., Lewis, S. L., Fisher, J. B., Lloyd, J., Lopez-Gonzalez, G., & Torres-Lezama, A. (2009). Drought sensitivity of the Amazon rainforest. Science, 323(5919), 1344-1347.

[17] Plumptre, A. J., Behangana, M., Ndomba, E., Davenport, T., Kahindo, C., Kityo, R., & Ssegawa, P. (2002). The biodiversity of the Albertine Rift. Wildlife Conservation Society Working Paper No. 19.

[18] Saleska, S. R., Didan, K., Huete, A. R., & da Rocha, H. R. (2007). Amazon forests green-up during 2005 drought. Science, 318(5850), 612.

[19] Sen, P. K. (1968). Estimates of the regression coefficient based on Kendall's tau. Journal of the American Statistical Association, 63(324), 1379-1389.

[20] Semazzi, F. H. M., & Song, Y. (2001). A GCM study of climate change induced by deforestation in Africa. Climate Research, 17(2), 169-182.

[21] Sibanda, M., Mutanga, O., & Rouget, M. (2023). Remote sensing of vegetation dynamics in African protected areas. Remote Sensing Applications: Society and Environment, 30, 100957.

[22] Still, C. J., Foster, P. N., & Schneider, S. H. (1999). Simulating the effects of climate change on tropical montane cloud forests. Nature, 398, 608-611.

[23] Tierney, J. E., Smerdon, J. E., Anchukaitis, K. J., & Seager, R. (2013). Multidecadal variability in East African hydroclimate controlled by the Indian Ocean. Nature, 493, 389-392.

[24] Tucker, C. J. (1979). Red and photographic infrared linear combinations for monitoring vegetation. Remote Sensing of Environment, 8(2), 127-150.

[25] Udahogora, M., Kayiranga, A., Muleta, D. B., & Nkurunziza, P. (2023). Assessment of land use and land cover change in Nyungwe National Park. Environmental and Sustainability Indicators, 18, 100235.

[26] Wagner, F. H., Herault, B., Bonal, D., Stahl, C., Anderson, L. O., Baker, T. R., & Galbraith, D. (2017). Climate seasonality limits leaf carbon assimilation and wood productivity in tropical forests. Biogeosciences, 13(8), 2537-2562.

[27] Zhu, Z., Piao, S., Myneni, R. B., Huang, M., Zeng, Z., Canadell, J. G., & Friedlingstein, P. (2016). Greening of the Earth and its drivers. Nature Climate Change, 6(8), 791-795.